Nuclear Environment in the Array of Loops ICRF Launcher Module of INTOR

Mohamed E. Sawan

May 1984

UWFDM-575

FUSION TECHNOLOGY INSTITUTE

UNIVERSITY OF WISCONSIN

MADISON WISCONSIN

Nuclear Environment in the Array of Loops ICRF Launcher Module of INTOR

Mohamed E. Sawan

Fusion Technology Institute
University of Wisconsin
1500 Engineering Drive
Madison, WI 53706

http://fti.neep.wisc.edu

May 1984

UWFDM-575

NUCLEAR ENVIRONMENT IN THE ARRAY OF LOOPS ICRF LAUNCHER MODULE OF INTOR

Mohamed E. Sawan

Fusion Engineering Program
Nuclear Engineering Department
University of Wisconsin-Madison
1500 Johnson Drive, Madison, WI 53706

May 1984

UWFDM-575

Abstract

Nuclear analysis for the array of loops ICRF launcher module design of INTOR is presented. The nuclear radiation environment in the different module components is determined. The fast neutron fluence in the BeO radome is 10^{22} n/cm^2 after one full power year leading to significant microcracking. Activation calculations for SF_6 imply a total activity of 5×10^4 Ci at shutdown. Nuclear heating results in a large breakdown rate in SF_6. A 1.6 m thick nuclear shield is needed to allow for hands-on maintenance one day after shutdown behind the launcher module.

1. Introduction

This report is aimed at determining the nuclear radiation environment in the 4 x 4 array of loops design proposed for ICRF launching in INTOR. Four launcher modules (2.4 m x 2.4 m each) are used with each module housing 16 element modules in a 4 x 4 array as shown in Fig. 1. The detailed configuration of the element module is shown also in Fig. 1 which was reproduced from Ref. 1. The BeO radome brazed to the launcher module frame establishes the vacuum boundary interface with the plasma chamber. Sulfur hexafluoride (SF_6) gas at atmospheric pressure is used behind this boundary to enhance the voltage holdoff characteristics of the loop and its transmission line. Each element module consists of the copper loop, the copper ground plane, two 3-3/8" diameter coaxial lines and a nuclear shield made of a box filled with steel balls and flushed with water. The element module nuclear shield is used to allow for hands-on maintenance 24 hours after shutdown. The neutronics analysis presented here gives an estimate for the required shield thickness.

The three-dimensional neutronics calculations have been performed in two steps. In the first step, the reactor cavity and fusion neutron source were modeled to yield the energy and angular distribution of neutrons and gamma photons incident on the front surface of the launcher module. In the second step of the calculations, the detailed geometrical configuration of the element module was modeled and neutron and gamma surface sources were used at the module front surface. The calculational models used in these two steps as well as the results of the calculations are given in the following sections.

2. Calculational Model for the Reactor Cavity

The MCNP[2] continuous energy coupled neutron-gamma Monte Carlo code was used to model the reactor geometry. Only 1/16 of the reactor was modeled with

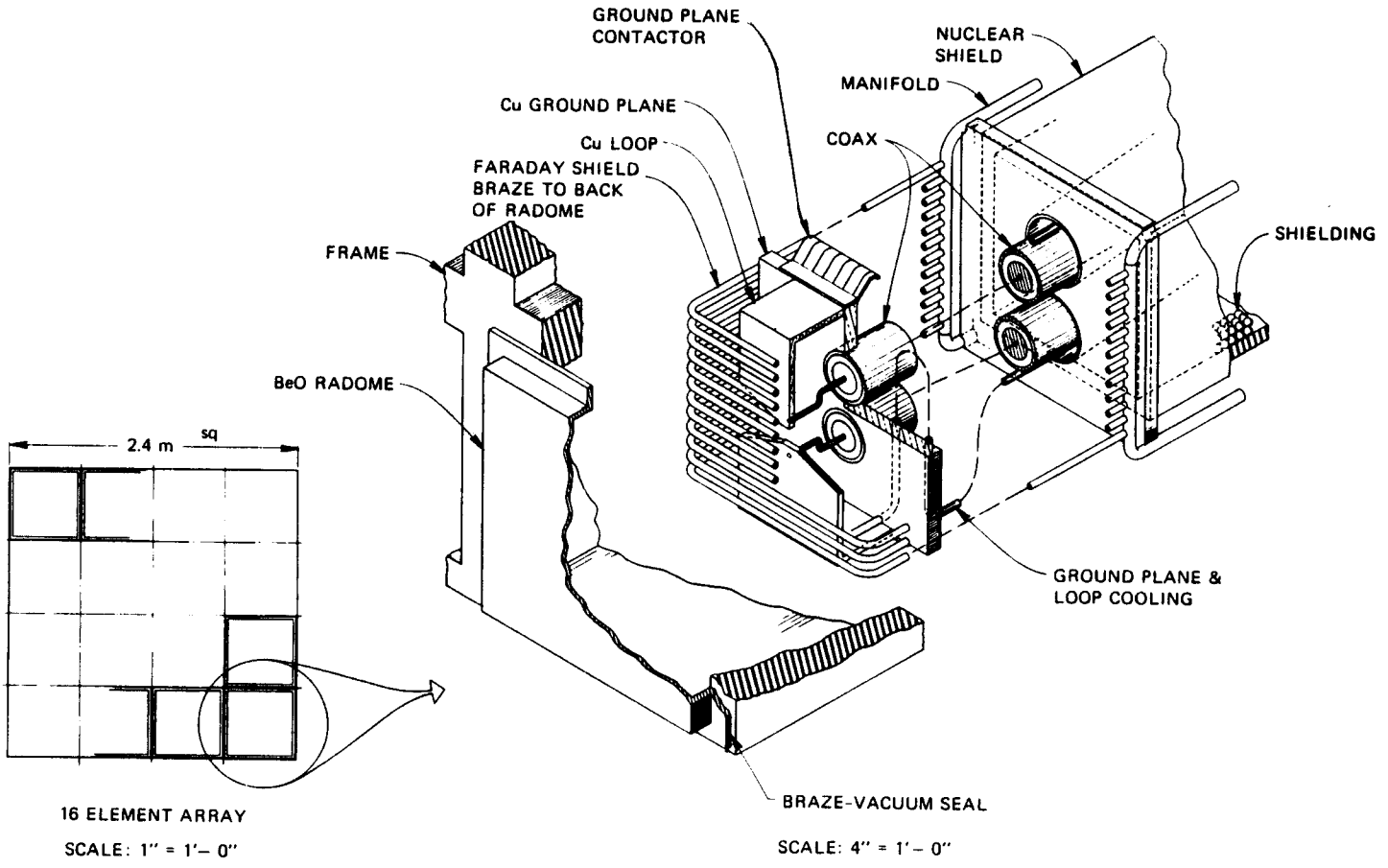

Fig. 1. The 4 x 4 ICRF launcher module with detailed configuration of the element module.

albedo reflecting surfaces used at the planes of symmetry. The model includes one-fourth of a launcher module. The vertical and horizontal cross sections of the geometrical model used in the calculations are given in Figs. 2 and 3. The plasma cavity was surrounded by a 60 cm thick reactor shield to properly account for neutrons and gamma photons reentering the cavity that could end up in the launcher module. This shield was assumed to consist of 80 vol.% Fe-1422 and 20 vol.% H_2O. The launcher module was divided into three zones. The front zone is 1 cm thick and represents the BeO radome. The second zone is 30 cm thick and consists of 30 vol.% SS, 15 vol.% Cu, 7 vol.% H_2O, 0.26 vol.% BeO, and 47.74 vol.% SF_6. The third zone is 90 cm thick and consists of 70.6 vol.% SS, 0.2 vol.% Cu, 0.5 vol.% BeO, 27.1 vol.% H_2O, and 1.6 vol.% SF_6. This zone represents the nuclear shield, the module frame and the coaxial lines. Since this model will be used only to determine the energy spectrum and angular distribution of neutrons and gamma photons incident on the front surface of the module, using average smeared densities in these zones will be adequate. The chamber major radius was taken to be 5.2 m with a width of 2.8 m at the midplane.

The D-shaped plasma zone boundary is given by the parametric equations

$$Z = a_0 \kappa \sin t \tag{1}$$

and

$$R = R_0 + a_0 \cos (t + 0.27 \sin t) . \tag{2}$$

The parameter t varies from 0 to π. The plasma major radius R_0, the plasma minor radius a_0, and the plasma elongation κ were taken to be 5.3 m, 1.2 m, and 1.6, respectively. This implies that at the midplane the scrapeoff zones

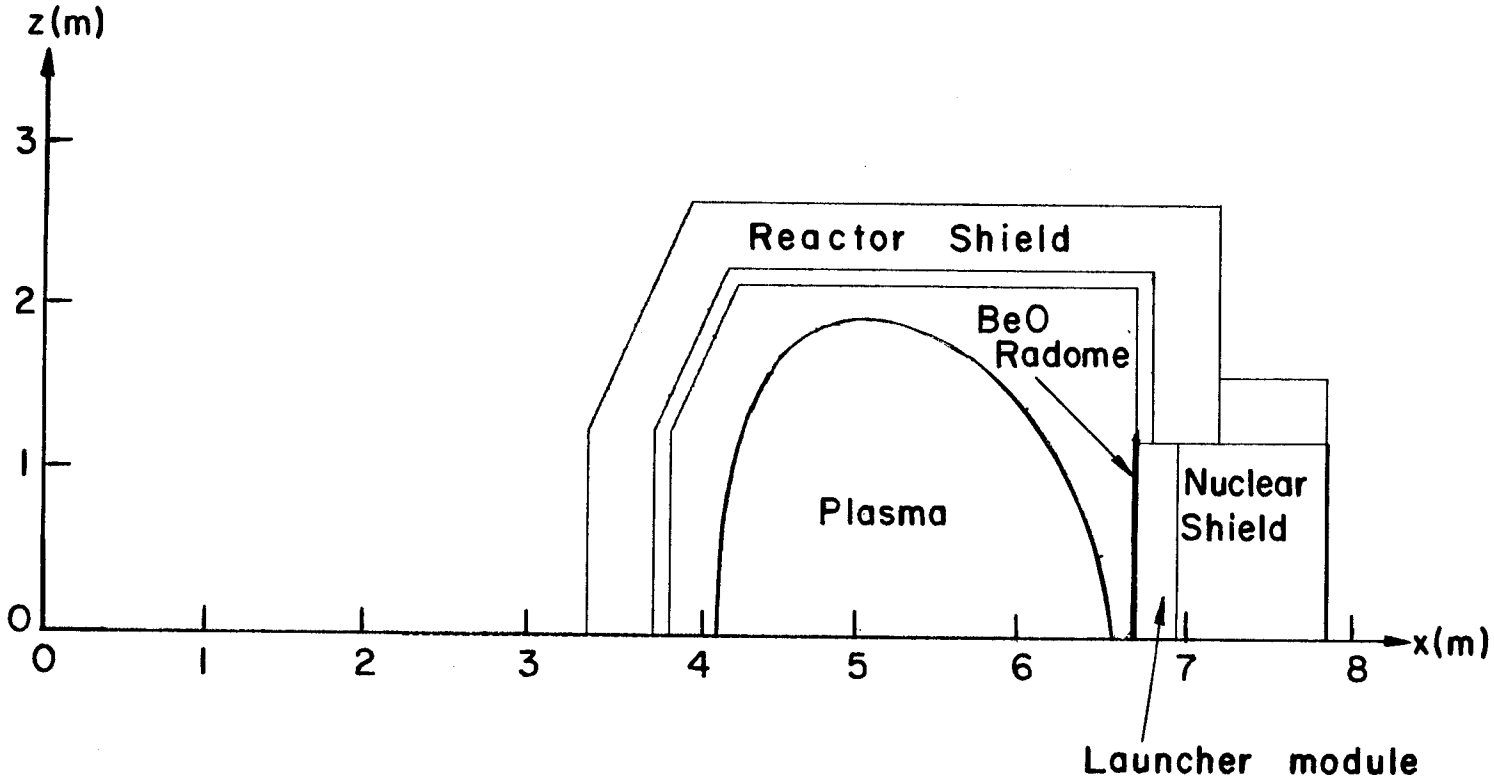

Fig. 2. Vertical cross section of the INTOR cavity geometrical model used in the calculations.

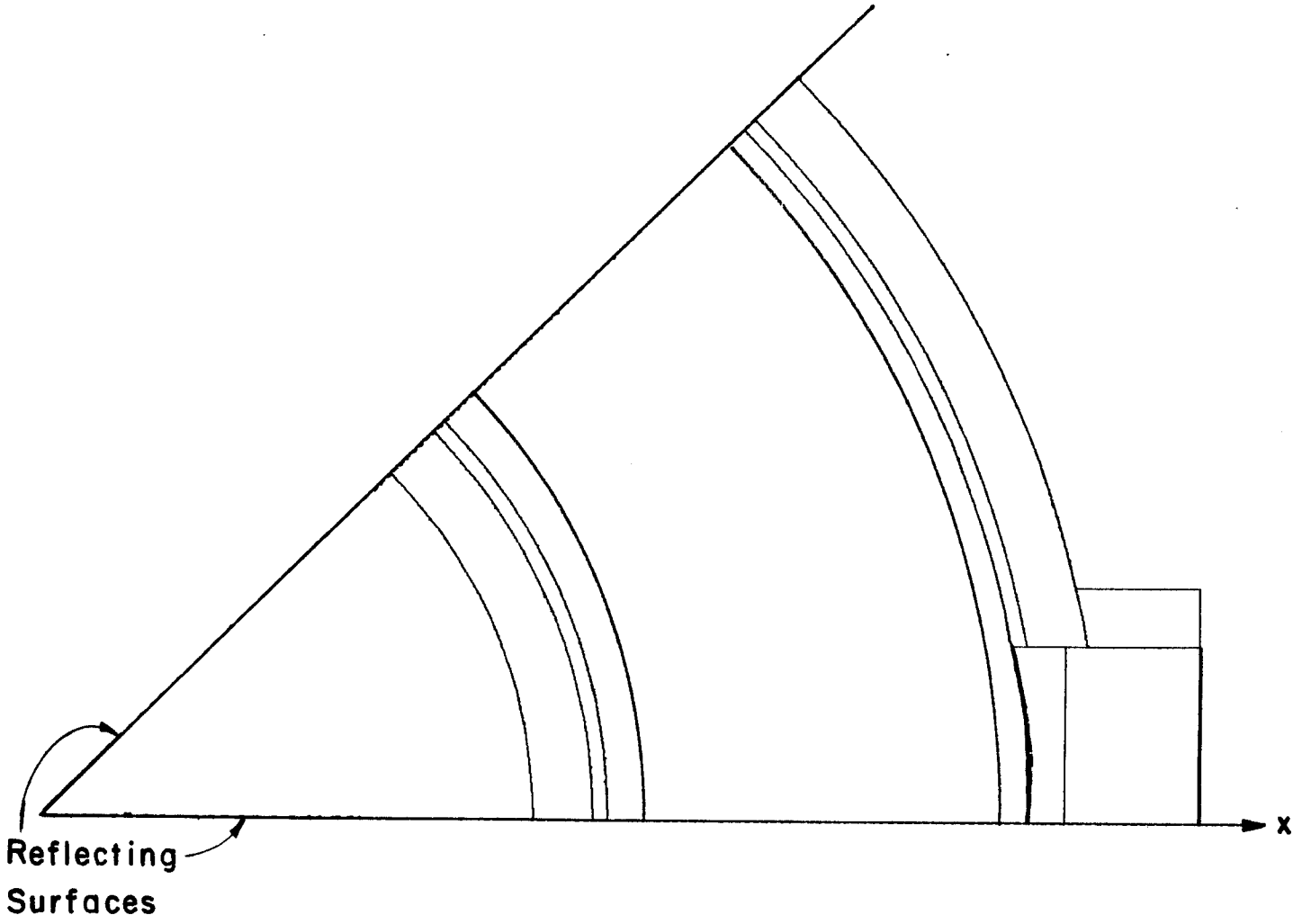

Fig. 3. Horizontal cross section of the INTOR cavity geometrical model used in the calculations.

are 10 cm and 30 cm thick on the outboard and inboard sides, respectively. The location of the neutron source was determined by sampling from the spatial source distribution

$$S(r,z) = S_o[1 - (r/r_m)^2]^2 \qquad (3)$$

where r is the distance between the source point and the magnetic axis (R = 5.45 m and Z = 0) and r_m is the distance measured from the magnetic axis to the plasma boundary passing through the source point.

Cross section data based on the ENDF/B-V evaluation were used in the calculations. A trapping surface was located at the interface between the launcher module and the plasma chamber. At this surface particles entering the module were counted according to energy and angle bins. Twenty thousand histories were used in the Monte Carlo calculations yielding statistical uncertainties less than 2% in the estimates for the number of neutrons and photons incident on the module front surface.

The same geometrical model shown in Figs. 2 and 3 was used in a separate Monte Carlo run to determine the poloidal variation of the neutron wall loading. In this run, no materials were used in the zones outside the plasma chamber. The uncollided neutrons crossing segmented zones of the plasma chamber boundary were tallied. 3×10^5 histories were used in this calculation yielding less than 1% statistical uncertainties in the calculated neutron wall loading at the different first wall segments.

3. Poloidal Variation of the Neutron Wall Loading

The poloidal variation of the neutron wall loading in INTOR as obtained from the Monte Carlo calculation is given in Fig. 4. The results are normal-

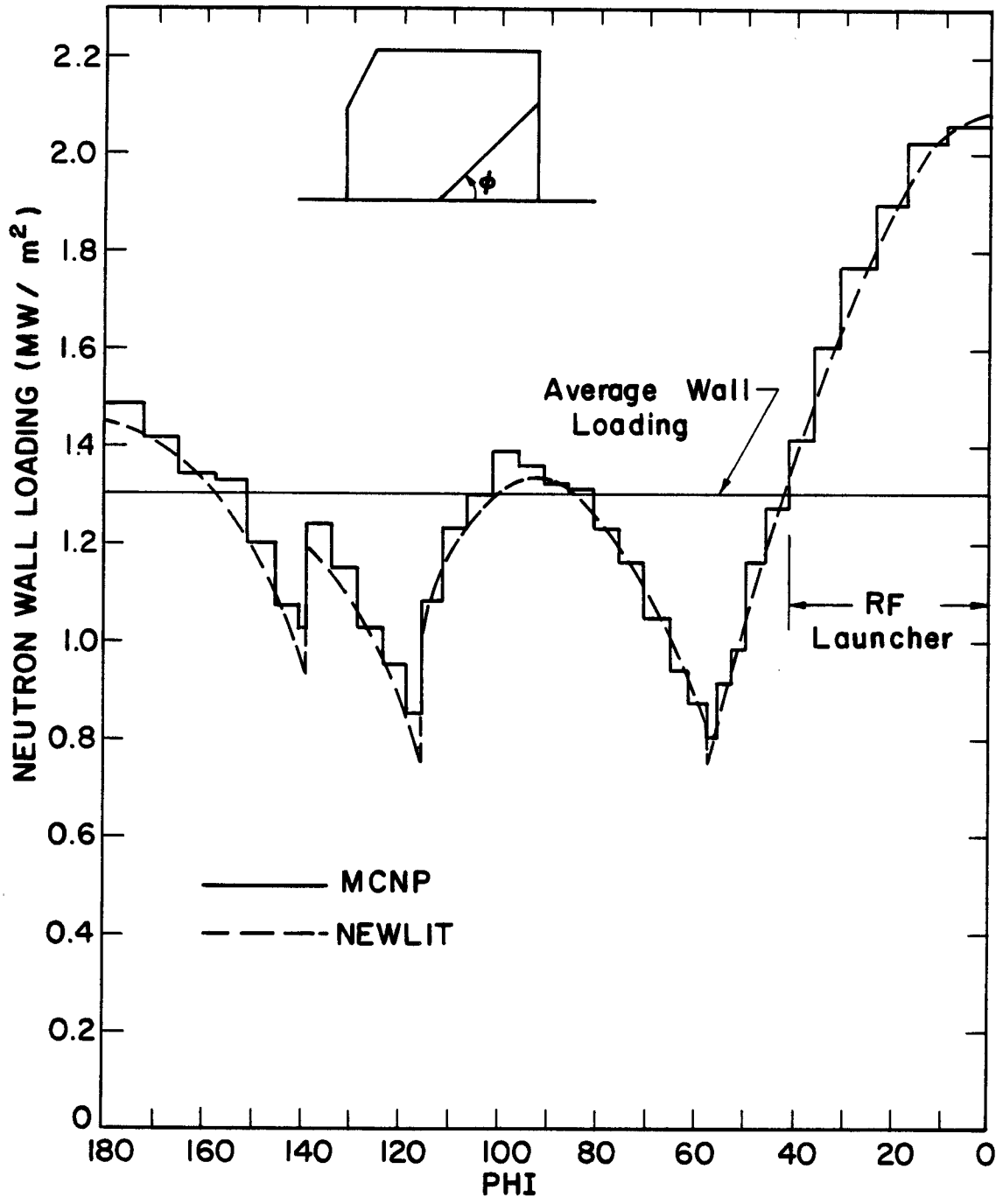

Fig. 4. Poloidal variation of neutron wall loading in INTOR as obtained by the MCNP and NEWLIT codes.

ized to an average neutron wall loading of 1.3 MW/m^2. The results indicate that a peak neutron wall loading of 2.07 MW/m^2 occurs at the reactor midplane on the outboard side. This significant peaking on the outboard side is attributed to the smaller scrapeoff zone (10 cm at outboard versus 30 cm at inboard), the outward shift of the peak neutron source in the plasma zone and the fact that the outboard part of the first wall sees more source neutrons than does the inboard part. The NEWLIT (NEutron Wall Loading In Torus) code was developed at the University of Wisconsin to calculate the poloidal variation of neutron wall loading in tokamak reactors for general plasma and first wall shapes[3] using ray tracing and numerical integration techniques. The code was used to calculate the neutron wall loading in INTOR. The results are shown in Fig. 5. The wall loading distribution in each segment of the first wall is indicated. The dashed line represents the average wall loading. The significantly peaked wall loading at the outboard side of the first wall is also evident from these results which are in excellent agreement with those obtained from MCNP as indicated in Fig. 4.

The results indicate that the front surface of the launcher module at the reactor midplane will be subjected to neutron wall loadings ~ 60% higher than the average reactor value. The average neutron wall loading at the front surface of the launcher module was calculated to be 1.8 MW/m^2 based on an average reactor value of 1.3 MW/m^2. Normalizing our results to a total fusion power of 620 MW, we obtained an average reactor wall loading of 1.1 MW/m^2 and a peak value of 1.76 MW/m^2 at the RF launcher module. Notice that while the average reactor wall loading could be sensitive to the first wall shape, the peak value is independent of the first wall shape provided that the location of the point at which the peak occurs relative to the plasma is unchanged. We

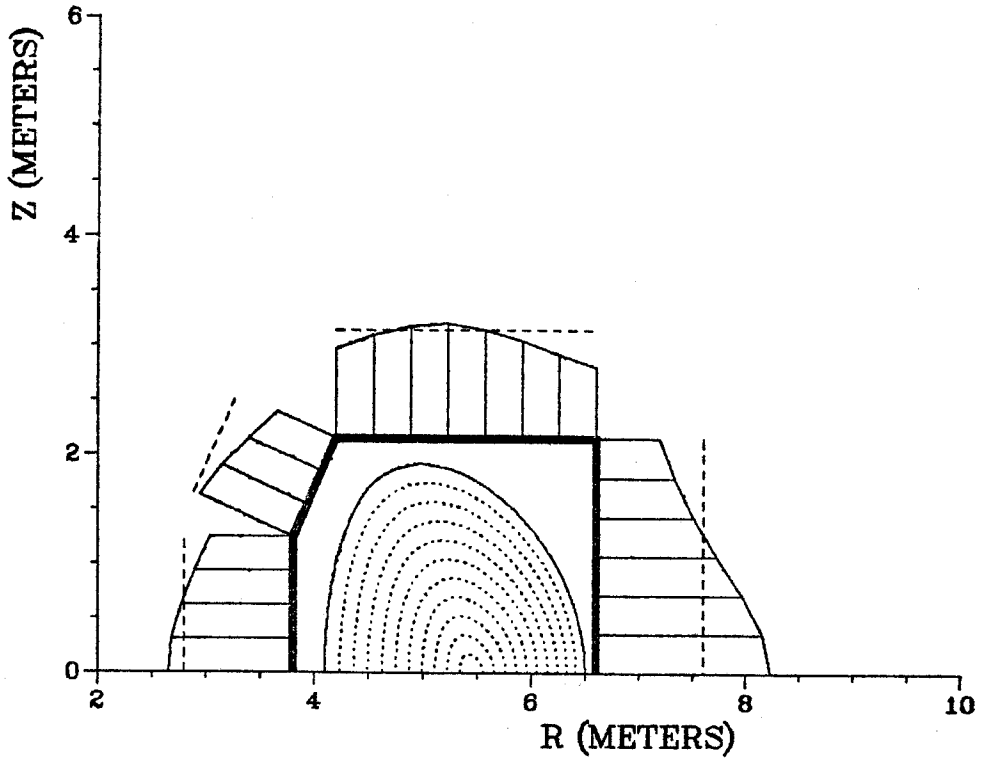

Fig. 5. Neutron wall loading distribution in INTOR obtained using the NEWLIT code.

conclude from the results presented here that the ICRF launcher modules in INTOR are subjected to an average neutron wall loading of 1.53 MW/m^2 and a peak value of 1.76 MW/m^2 at the reactor midplane.

4. Nuclear Radiation Incident on Launcher Module

The energy spectra of neutrons and gamma photons incident on the front surface of the ICRF launcher module are shown in Fig. 6. The results are normalized to an average neutron wall loading of 1 MW/m^2 at the module front surface. The results were obtained for energy bins that correspond to the 30 neutron-12 gamma LANL group structure. The calculations indicated that for one fusion source neutron generated in the plasma zone, 0.0745 source neutrons will impinge directly on the module front surface while a total of 0.151 neutrons (collided and uncollided) will be incident on the surface. Hence, the uncollided neutrons impinging directly on the module front surface represent ~ 50% of the total impinging neutrons which average 7.5 MeV in energy. For one fusion source neutron generated in the plasma zone, our results indicate that 0.063 gamma photons produced from neutron interactions in the materials surrounding the plasma chamber will end up impinging on the module front surface. The average energy of these photons is 1.7 MeV.

The angular distributions of neutrons and gamma photons incident on the module front surface are given in Fig. 7. The results are normalized to a unit average neutron wall loading at this surface. The angle θ is measured from the normal to the surface. It is clear that the angular distribution peaks at normal incidence. The results of Figs. 6 and 7 were stored to serve as source distributions in later modeling of the launcher element module itself.

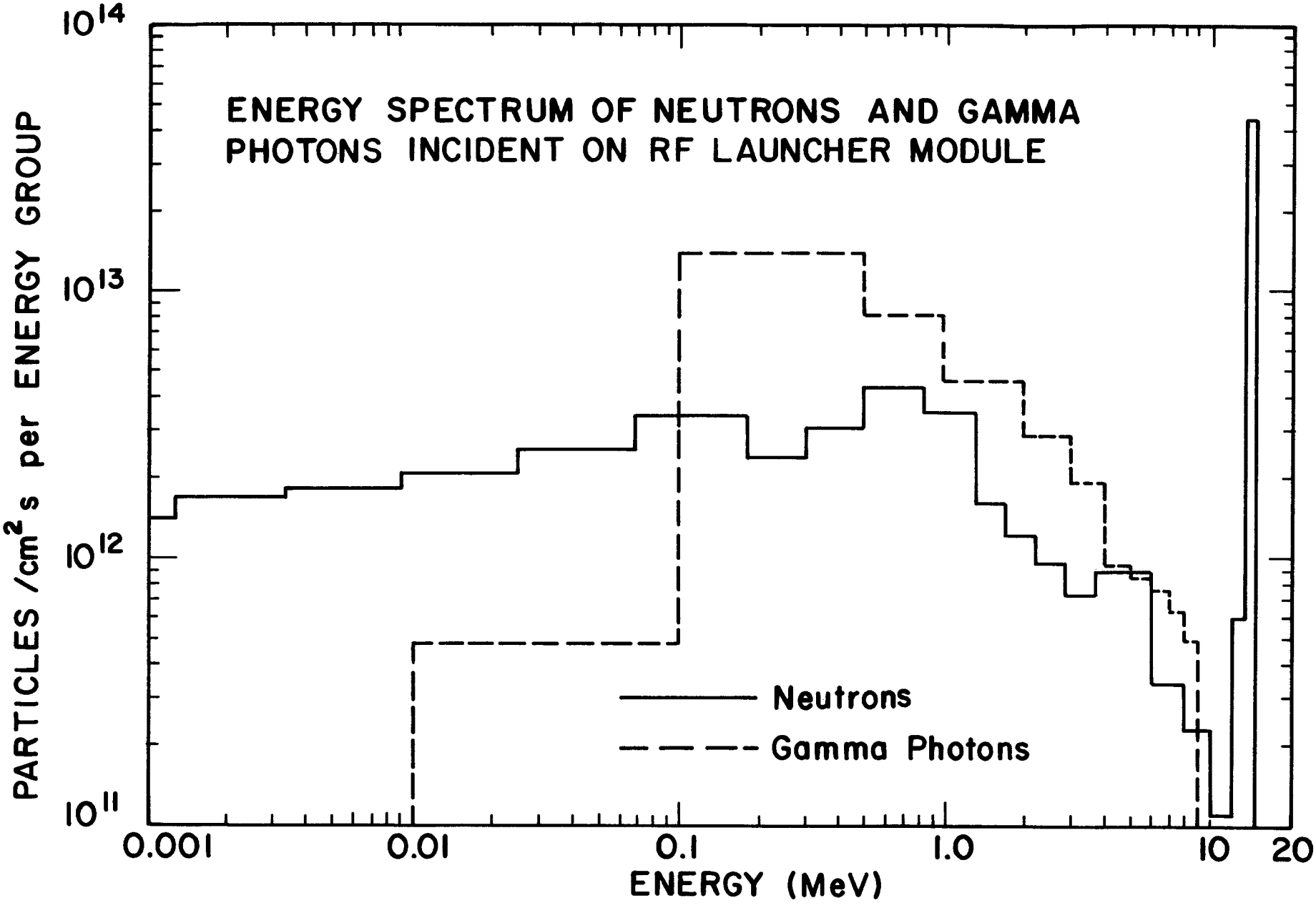

Fig. 6. Energy spectra of neutrons and gamma photons incident on the front surface of the launcher module.

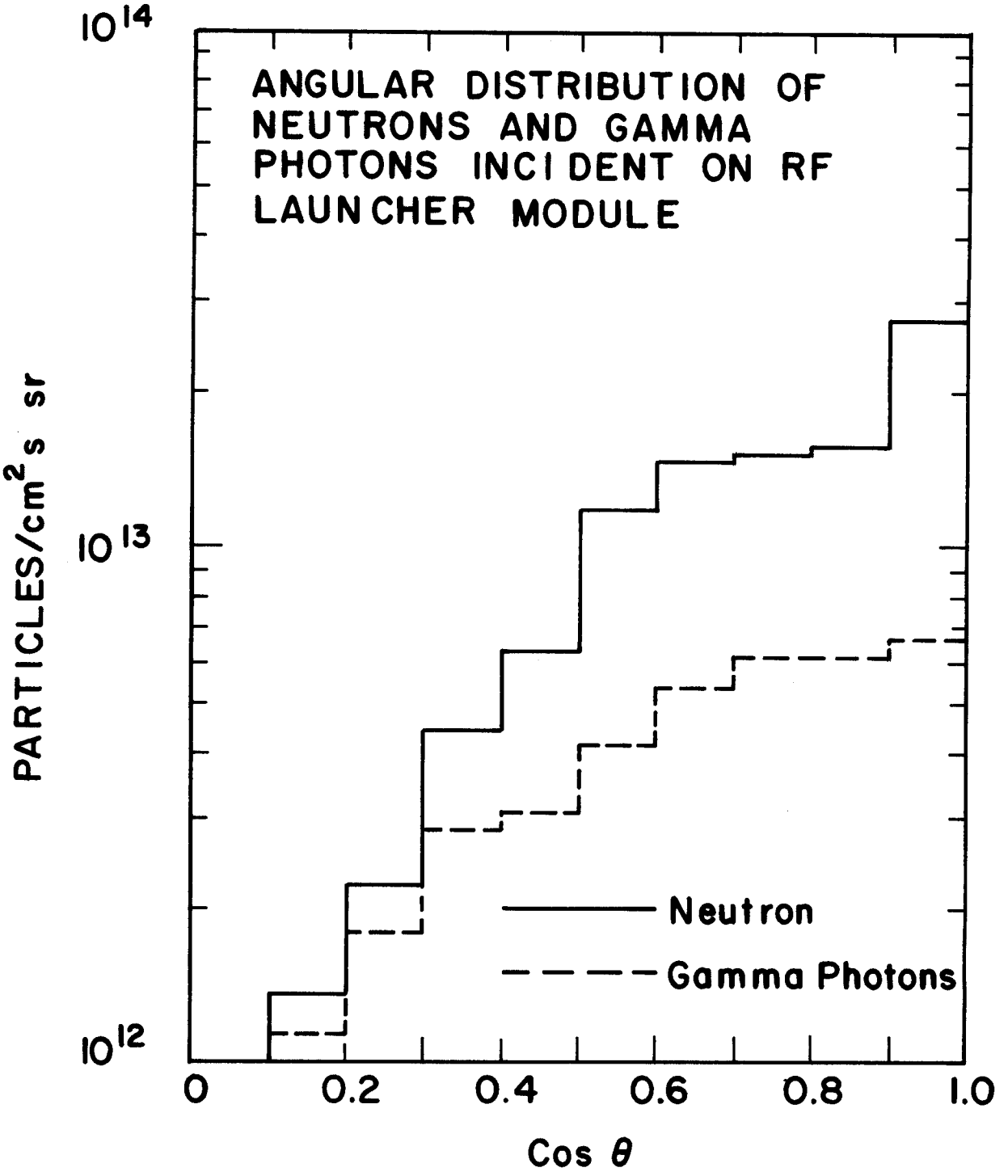

Fig. 7. Angular distribution of neutrons and gamma photons incident on the module front surface.

5. Calculational Model for the Launcher Element Module

Because of symmetry, only one-fourth of an element module was modeled for the MCNP calculations. Figures 8 through 13 give different geometrical cross sections in the model showing the different components. Reflecting boundaries were used at the planes z = 0, z = 30 cm, y = 0, and y = 30 cm to account for the geometrical symmetry. Although the model does not account for the blanket and shield adjacent to the launcher module, it gives appropriate representation of the conditions at the central element module where the end effects are insignificant and where the worst radiation environment exists due to the peaked neutron wall loading.

The model is an idealization and adaptation of the actual launcher design. The BeO radome was assumed to have a thickness of 1 cm followed by a 0.75 cm thick Faraday shield. The loop was assumed to have a thickness of 1 cm while the ground plane is 2 cm thick. The loop and ground plane coolant zones are 0.75 cm thick. The coaxial line has a central copper tube with inner and outer diameters of 3.12 and 3.34 cm, respectively, and is filled with water. The outer copper tube has inner and outer diameters of 7.68 and 7.94 cm, respectively. The space between the two coaxial conductors is occupied by BeO spacers and SF_6 gas. The coaxial cables go through two right angle bends, as shown in Fig. 8, to reduce radiation streaming to the back of the nuclear shield. A nuclear shield thickness of 90 cm was used in the calculations. Table 1 gives the composition and nuclide densities used in the different zones.

Two separate calculations have been performed. The first one is a coupled neutron-photon calculation with a neutron surface source at the module front surface having the energy and angular distributions given in Figs. 6 and

Table 1. Composition and Nuclide Densities Used in the Different Zones

Zone	Volumetric Composition	Mass Density g/cm^3	Nuclide Density nuclei/b•cm
Radome	100% BeO	3.03	Be 0.07287 O 0.07287
Launcher Module Frame	100% Type 316 SS	7.8	Fe 0.0546 Cr 0.0152 Ni 0.0112 Mo 0.0014 Mn 0.00123
Faraday Shield & Coolant Serpentine Tubes	10% Cu 40% H_2O	1.3	Cu 0.0085 H 0.0268 O 0.0134
Loop, Ground Plane & Coax Conductors	100% Cu	8.96	Cu 0.0849
Coax Coolant	100% H_2O	1	H 0.0669 O 0.0334
Space Between Coax Conductors	10% BeO 90% SF_6	0.31	Be 0.0073 O 0.0073 S 1.55×10^{-5} F 9.36×10^{-5}
SF_6 Gas	100% SF_6	4.2×10^{-3}	S 1.72×10^{-5} F 1.04×10^{-4}
Element Module Nuclear Shield	60% Fe 1422 40% H_2O	5.18	Fe 0.0420 Mn 7.30×10^{-3} C 1.39×10^{-3} Cr 1.11×10^{-3} Ni 9.48×10^{-4} H 0.0268 O 0.0134

Fig. 8. Vertical cross section of the element module geometrical model used in the Monte Carlo calculations.

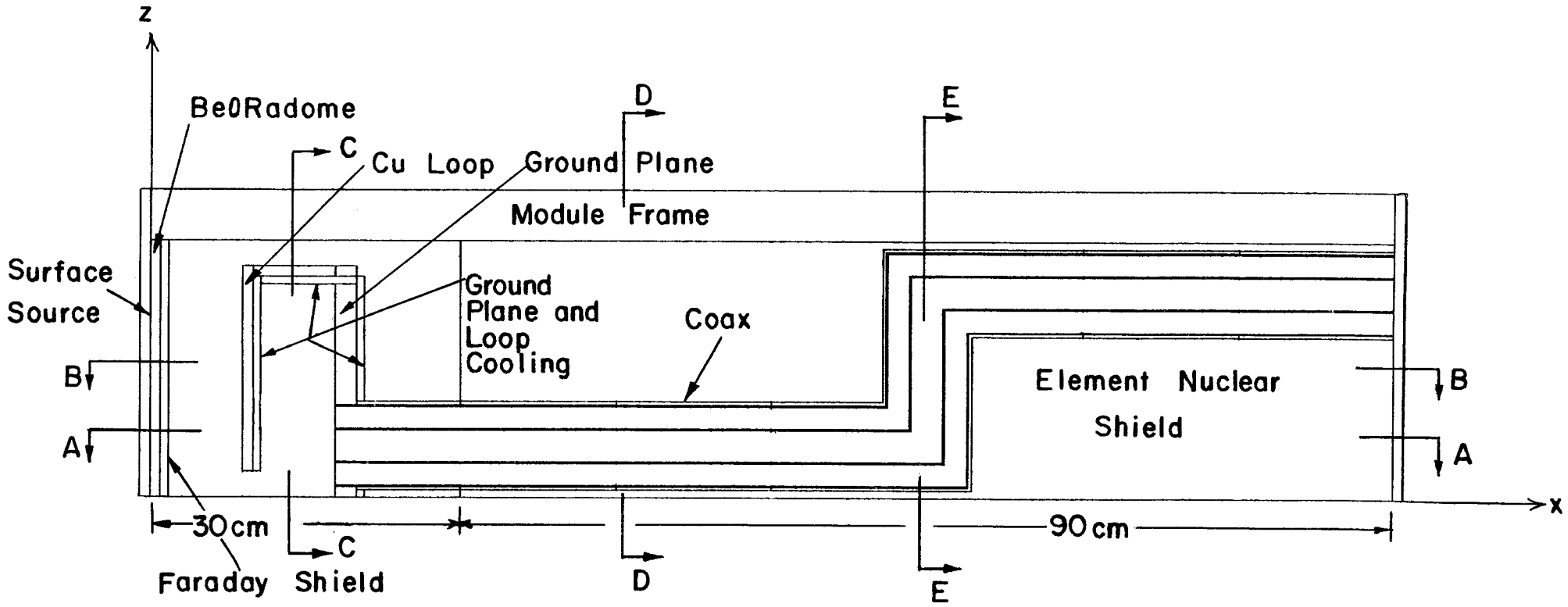

Fig. 9. Section A-A of the geometrical model.

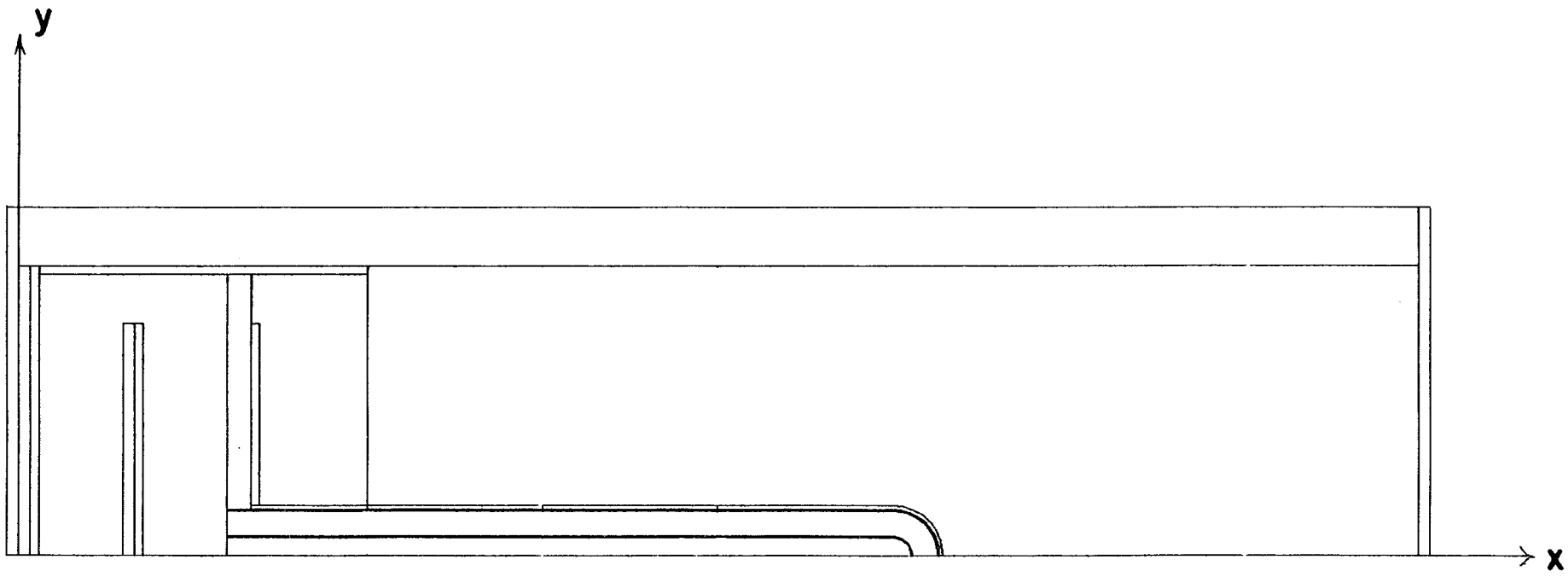

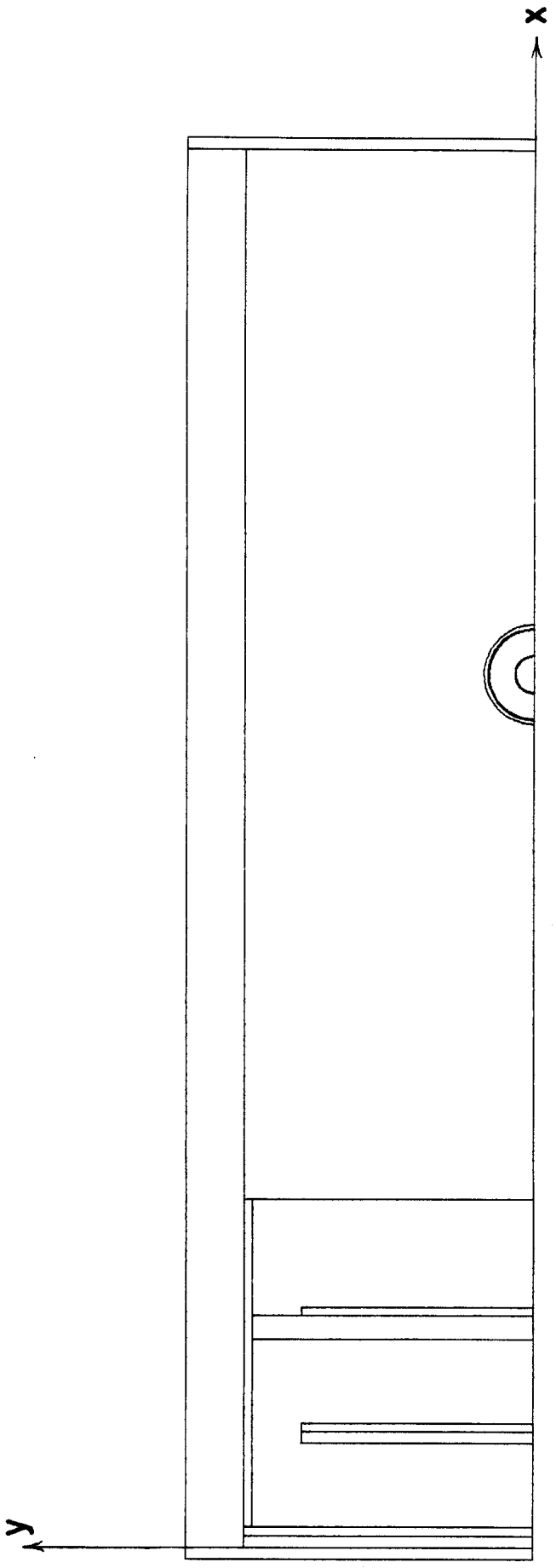

Fig. 10. Section B-B of the geometrical model.

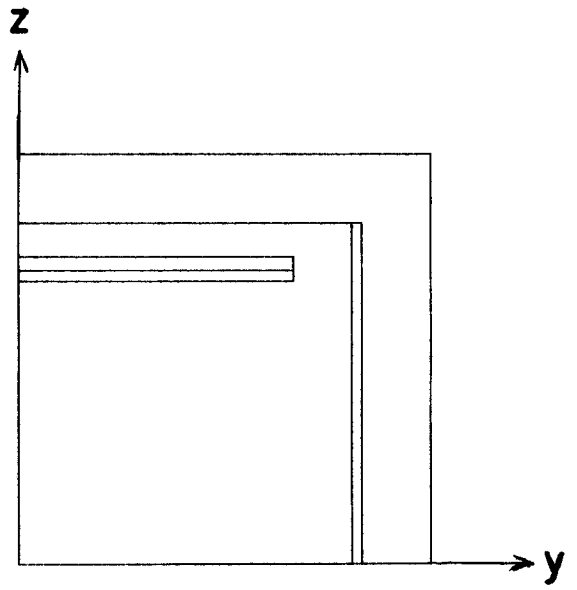

Fig. 11. Section C-C of the geometrical model.

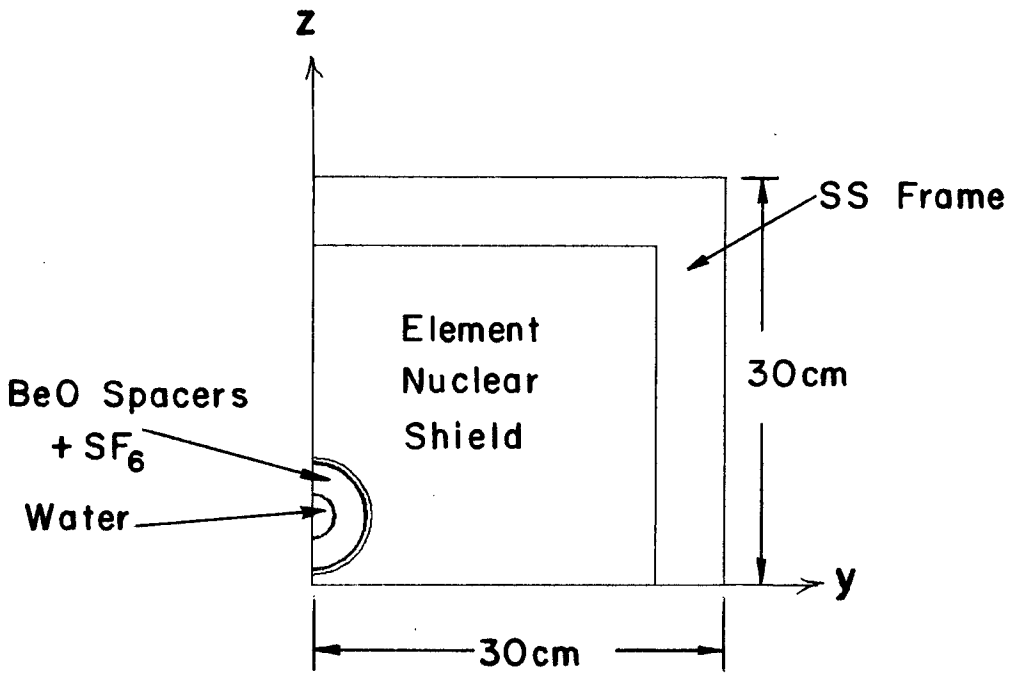

Fig. 12. Section D-D of the geometrical model.

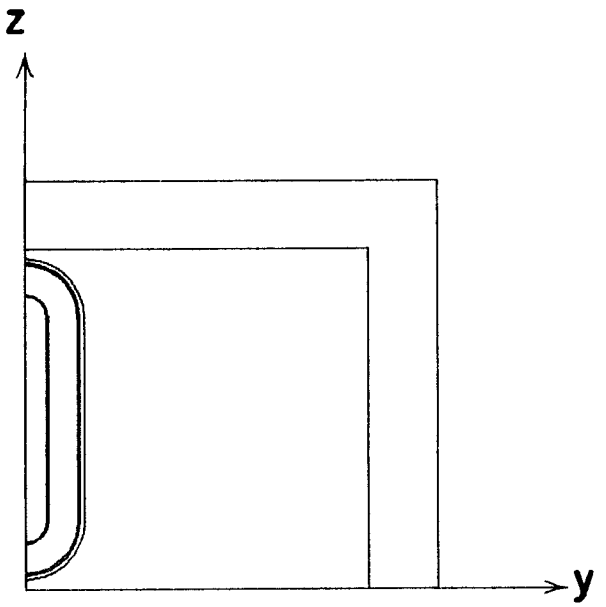

Fig. 13. Section E-E of the geometrical model.

7. The second calculation is a photon only calculation in which a photon surface source at the module front surface is sampled from the gamma energy and angular distributions of Figs. 6 and 7. The results of the two calculations were added to get the contribution from both neutron and gamma surface sources. MCNP runs of 10,000 and 20,000 histories were carried out for the first and second calculations, respectively, with cross section data based on the ENDF/B-V evaluation. Different variance reduction techniques were used to improve the accuracy of the calculation. Geometry splitting with Russian roulette was used to split the particles as they moved away from the source towards the back of the shield. The statistical uncertainty in the neutron related responses varied from ~ 1% in zones near the source to ~ 30% at the back of the shield. The corresponding values for the gamma related quantities are ~ 2% and 24%, respectively.

6. Nuclear Radiation Parameters in Radome and BeO Spacers

Due to its good rf power transparency and thermal conductivity, BeO was proposed for use as the ceramic element module radome that forms the interface with the plasma chamber. We calculated the nuclear radiation environment at the BeO radome as well as some relevant radiation damage parameters. The results normalized to a unit wall loading are given in Table 2.

For a peak neutron wall loading of 1.76 MW/m^2 at the launcher module, the BeO radome will be subjected to a peak fast neutron fluence of 10^{22} n/cm^2 ($E > 0.1$ MeV) after one year of full operation. The radiation effect of greatest concern in BeO is microcracking that results from the anisotropy of lattice expansion. Microcracking will lead to severe degradation of strength. Since the radome serves as a vacuum boundary, the radiation induced microcracking will limit its life. Data obtained for samples irradiated in fission reactor

Table 2. Nuclear Radiation Parameters in the BeO Radome for 1 MW/m^2 Wall Loading

Neutron flux	2.8×10^{14} $n/cm^2 \cdot s$
Gamma flux	1.53×10^{14} $\gamma/cm^2 \cdot s$
Fast neutron fluence (E > 0.1 MeV) after one full power year (FPY)	5.77×10^{21} n/cm^2
Helium production	431 appm/FPY
Hydrogen production	93 appm/FPY
Tritium production	20 appm/FPY
Power density	8.53 W/cm^3
Absorbed dose rate	8.9×10^{12} rad/FPY

neutron environments indicate that the onset of microcracking occurs at fluences of 10^{20}-10^{21} n/cm^2 (E > 0.1 MeV) at temperatures below 300°C.[4] The onset fluence decreases as the temperature decreases. The temperature on the radome surface in the present launcher module design is expected to be around 160°C. Considering a fluence limit of 10^{20} n/cm^2, our results indicate that the BeO radome has to be changed every 0.01 FPY. The lower fluence limit was considered to account for lower operating temperatures and the fact that neutrons with a degraded fusion spectrum produce more damage than does the same number of neutrons with a fission spectrum. Use of other candidate ceramics that can tolerate higher neutron fluences such as alumina (Al_2O_3) and spinel ($MgAl_2O_4$) must be thoroughly investigated. The results given in Table 2 can also be used to assess other irradiation effects that might influence the operation of the launcher such as gas production and electrical resistivity degradation.

BeO is used also as a spacer between the central and return conductors of the coaxial line. Table 3 gives the nuclear radiation parameters for the BeO spacers averaged over segmented zones of the coax. The results are normalized to unit wall loading at the front surface of the launcher module. These results indicate that the BeO spacers in the front part of the coax will be subjected to high neutron fluences that might result in microcracking after a short time of operation.

7. Nuclear Radiation Environment at the Loop, Ground Plane and Transmission Lines

The nuclear radiation environment at the loop, ground plane, and coaxial lines has been determined. In this calculation copper was used. Although other candidate materials can be used, the neutron and gamma fluxes calculated

Table 3. Nuclear Radiation Parameters in the BeO Spacers of the Coax for 1 MW/m^2

Distance From the Front Surface of the Launcher Module (m)	Neutron Flux ($n/cm^2 \cdot s$)	Gamma Flux ($\gamma/cm^2 \cdot s$)	Fast Neutron Fluence After 1 FPY (n/cm^2)	He Production appm/FPY	H Production appm/FPY	T Production appm/FPY	Power Density (W/cm^3)	Absorbed Dose Rate (rad/FPY)
0.18-0.30	1.98×10^{14}	1.18×10^{14}	2.96×10^{21}	144	29.4	6.56	4.12	4.3×10^{12}
0.30-0.45	9.92×10^{13}	7.67×10^{13}	1.39×10^{21}	70	13.4	3.01	2.35	2.45×10^{12}
0.45-0.60	2.38×10^{13}	2.39×10^{13}	3.07×10^{20}	16.6	3.25	0.71	0.65	6.78×10^{11}
0.60-0.90	7.18×10^{12}	3.23×10^{12}	2.86×10^{19}	1.8	0.34	0.072	0.08	8.34×10^{10}
0.90-1.05	2.54×10^{11}	2.66×10^{11}	3.53×10^{18}	0.1	0.02	0.0046	0.0059	6.15×10^{9}
1.05-1.20	2.32×10^{10}	4.31×10^{10}	1.55×10^{17}	0.002	0.0004	0.00002	5.76×10^{-4}	6.01×10^{8}

here are not sensitive to the material choice and can still be used as an indication of the nuclear environment. However, the nuclear heating values will significantly depend on the material used. Table 4 gives the neutron and gamma fluxes as well as the power density in different zones of the loop, ground plane, and central and return conductors of the coaxial line. The results are normalized to unit wall loading at the front surface of the launcher module. Degradation of copper conductivity as a result of irradiation is a concern which needs to be assessed using the calculated nuclear environment.

8. Activation of the Sulfur Hexafluoride Gas

The level of activity of the SF_6 gas in the launcher module of INTOR has been determined using the DKR code.[5] The code used the neutron spectra obtained from the MCNP Monte Carlo calculation in the different zones of the module. The zone between the BeO radome and the nuclear shield was divided into three segments and the average neutron flux in each segment was used in the DKR calculations. The front segment extends from the radome to the front of the loop. The next segment extends from the loop to the ground plane while the last segment extends from the ground plane to the front surface of the nuclear shield. The flux in a 0.5 cm thick region behind the radome was used in the calculations to determine the peak activation level in the SF_6 gas. Activation of the SF_6 gas used in the space between the two conductors of the coax was neglected due to the significant degradation of the neutron flux and the small volume of gas used in this region. An operating time of one full power year at a neutron wall loading of 1 MW/m^2 was used. The specific activities in Ci/cm^3 at shutdown in the three segments as well as the peak activity are given in Table 5. The contributions from the different radioisotopes are indicated.

Table 4. Nuclear Radiation Parameters in the Loop, Ground Plane and Coaxial Line for 1 MW/m^2

Component	Distance From Front Surface of Module (m)	Neutron Flux ($n/cm^2 \cdot s$)	Gamma Flux ($\gamma/cm^2 \cdot s$)	Fast Neutron Fluence ($E > 0.1$ MeV) After 1 FPY (n/cm^2)	Power Density (W/cm^3)		
					n	γ	Total
Loop							
Front	0.09-0.10	2.61×10^{14}	1.26×10^{14}	5.25×10^{21}	0.87	8.58	9.45
Top	0.10-0.18	2.28×10^{14}	1.34×10^{14}	4.48×10^{21}	0.54	6.98	7.52
Ground Plane	0.18-0.20	2.19×10^{14}	1.33×10^{14}	4.09×10^{21}	0.55	7.29	7.84
Central Conductor in Coax	0.18-0.30	1.76×10^{14}	1.18×10^{13}	2.61×10^{21}	0.38	7.25	7.63
	0.30-0.45	1.04×10^{14}	7.61×10^{13}	1.39×10^{21}	0.25	4.77	5.02
	0.45-0.60	2.29×10^{13}	2.32×10^{13}	2.92×10^{20}	0.082	1.61	1.692
	0.60-0.90	1.69×10^{12}	2.55×10^{17}	2.05×10^{19}	0.0047	0.16	0.165
	0.90-1.05	2.04×10^{11}	2.20×10^{11}	2.48×10^{18}	0.00015	0.0157	0.0159
	1.05-1.20	1.22×10^{10}	7.10×10^{10}	1.40×10^{17}	1.2×10^{-5}	0.0054	0.0054
Return Conductor in Coax	0.18-0.30	1.84×10^{14}	1.21×10^{14}	3.12×10^{21}	0.52	7.39	7.91
	0.30-0.45	9.67×10^{14}	7.91×10^{13}	1.31×10^{21}	0.23	5.20	5.43
	0.45-0.60	2.28×10^{13}	2.41×10^{13}	3.08×10^{20}	0.065	1.66	1.725
	0.60-0.90	2.22×10^{12}	2.91×10^{12}	3.02×10^{19}	0.008	0.19	0.198
	0.90-1.05	1.88×10^{11}	2.14×10^{11}	2.14×10^{18}	0.00022	0.011	0.0112
	1.05-1.20	2.15×10^{10}	6.80×10^{10}	1.30×10^{17}	4.6×10^{-5}	0.0027	0.00275

Table 5. Activity (Ci/cm^3) of SF_6 Gas in the Launcher Module for 1 MWy/m^2 at Shutdown

Isotope	Half-Life	Peak	Segment 1 (1 cm < x < 9 cm)	Segment 2 (9 cm < x < 18 cm)	Segment 3 (18 cm < x < 30 cm)
^{16}N	7.2 s	8.901-3[a]	5.430-3	2.054-3	8.747-4
^{19}O	29 s	3.868-3	2.136-3	7.714-4	2.983-4
^{18}F	109.7 m	9.155-3	4.710-3	1.597-3	5.655-4
^{20}F	11.4 s	9.920-4	1.001-3	7.048-4	4.341-4
^{32}P	14.3 d	8.246-3	4.923-3	1.832-3	7.661-4
^{33}P	25.3 d	8.295-5	4.874-5	1.836-5	7.674-6
^{31}Si	2.62 h	1.040-4	5.508-5	1.951-5	7.443-6
^{35}S	88 d	6.666-5	6.240-5	4.516-5	2.882-5
^{37}S	5.06 m	1.403-7	1.316-7	9.526-8	6.082-8
Total		3.142-2	1.837-2	7.042-3	2.983-3

[a]Reads 8.901×10^{-3}

It can be seen that within three minutes, three of the isotopes (^{16}N, ^{19}O and ^{20}F) will decay away leaving ^{18}F and ^{32}P as the dominant isotopes. From 1 day to 120 days after shutdown, ^{32}P dominates and after 120 days ^{35}S will be the dominant source of activity. The total activity will be down by four orders of magnitude within one year after shutdown.

Using the volumes for the segmented zones of SF_6 gas in the module and considering a peak neutron wall loading of 1.76 MW/m^2 we estimated that 893 Ci of SF_6 activity in the element module at the reactor midplane needs to be handled immediately after shutdown. One day after shutdown this activity level will reduce to 229 Ci. Using the average launcher module wall loading of 1.53 MW/m^2 we estimated that the total SF_6 activity in the launcher module consisting of 16 elements is 1.26×10^4 Ci after shutdown and 3.22×10^3 Ci one day later. Since four modules are used in INTOR, this amounts to a total SF_6 activity of 5×10^4 Ci after shutdown and 1.3×10^4 Ci one day later.

9. Radiation Chemistry of the Sulfur Hexafluoride Gas

Table 6 gives the neutron and gamma fluxes as well as nuclear heating in the SF_6 gas used in the launcher module. The results are normalized to unit wall loading at the front surface of the launcher and are given for different zones. These results can be used to determine the breakdown rate of SF_6 due to nuclear heating. Although breakdown products do not reduce the dielectric strength, they are extremely reactive. The corrosive nature of the breakdown products is of particular concern in accelerators where the concentration of these products must be kept at low levels by recirculation through purification systems.[6] Using a peak wall loading of 1.76 MW/m^2, the results of Table 6 indicate that the average energy deposition rate in the SF_6 gas of the element module at the reactor midplane is 13.84 mW/cm^3. Using the G-factor,

Table 6. Nuclear Parameters in the SF_6 Gas for 1 MW/m^2

Region	Distance From Front Surface of Module (m)	Flux (cm^{-2} s^{-1})		Power Density (mW/cm^3)		
		Neutron	Gamma	Neutron	Gamma	Total
Loop Region	0.01-0.09	2.74(14)[a]	1.52(14)	8.17	3.12	11.29
	0.09-0.18	7.40(14)	1.39(14)	5.46	2.81	8.27
	0.18-0.30	1.83914)	1.02(14)	2.95	2.26	5.21
Coax Region	0.18-0.30	1.89(14)	1.18(14)	3.68	2.69	6.37
	0.30-0.45	9.92(13)	7.67(13)	1.79	1.80	3.59
	0.45-0.60	2.38(13)	2.39(13)	0.39	0.58	0.97
	0.60-0.90	2.18(12)	3.23(12)	0.05	0.07	0.12
	0.90-1.05	2.54(11)	2.66(11)	0.003	0.006	0.009
	1.05-1.20	2.32(10)	4.31(10)	0.00009	0.00068	0.00077

[a]Reads 2.74×10^{14}

defined as the number of breakdown product molecules formed per 100 eV absorbed radiation, one can calculate the breakdown product production rate. No G-factor was measured for SF_6. We assumed that the breakdown of SF_6 by irradiation into $SF_4 + F_2$ is similar to the formation of H_2 by gamma irradiation of ethane which has a G-factor of 6.8.[7] This implies that 5.88×10^{15} breakdown product molecules will be formed per cm^3 per second which represent 0.034% of the original number of SF_6 molecules. This extremely high breakdown product production rate based only on nuclear heating will require continuous recirculation through purification systems.

10. Radiation Environment Behind the Nuclear Shield

Each element module of the launcher module has a nuclear shield behind it to allow for hands-on maintenance 24 hours after shutdown. Shutdown gamma radiation originates from induced activation in the outer layers of the shield and in unshielded equipment behind the shield. Earlier work on ETF and FED indicated that activation of shield and outlying components will be low enough to result in a general shutdown dose rate of 2.5 mrem/hr one day after shutdown if the neutron flux at the back of the shield is kept at a level of $\sim 2 \times 10^6$ $n/cm^2 \cdot s$ during operation.

The results of the neutronics calculations for the launcher module indicate that the average neutron flux behind a 0.9 m thick shield is 1.81×10^9 $n/cm^2 \cdot s$ with a peak value of 1.37×10^{10} $n/cm^2 \cdot s$ at the exit of the coax. These values were normalized to a unit wall loading. Given a peak wall loading of 1.76 MW/m^2 we estimated that a total shield thickness of $\sim$ 1.6 m is required to reduce the neutron leakage flux to an acceptable level of $\sim 10^6$ $n/cm^2 \cdot s$.

11. Nuclear Heat Load in the Module

Nuclear heating resulting from both neutron and gamma energy deposition was calculated in the different components of the module. The nuclear heat loads in kW are given in Table 7. The results are given for one quarter of the element module (1/64 of the launcher module) and are normalized to unit neutron wall loading. Based on a peak neutron wall loading of 1.76 MW/m^2, a power of 102 kW resulting from nuclear heating should be handled by the loop and ground plane coolant in each element module at the reactor midplane. Only 8 kW of nuclear heat is to be removed by the coolant in the two coaxial lines of the element module. Using the average launcher module wall loading of 1.53 MW/m^2 we calculated the total power from nuclear heating in all four launcher modules to be 45 MW. About 47% of this power comes from nuclear heating in the module frame and 15% from nuclear heating in the nuclear shield. The remaining power results from nuclear heating in the different launcher components. Notice that the additional nuclear heating resulting from increasing the shield thickness by 70 cm as suggested in the previous section is negligible as the flux in the back part of the shield is several orders of magnitude lower than that in the front part of the shield.

12. Summary

Nuclear analysis has been performed for the ICRF launcher module of INTOR consisting of a 4 x 4 array of loops. The poloidal variation of neutron wall loading in INTOR was determined. The results indicate that the launcher modules are subjected to an average neutron wall loading of 1.52 MW/m^2 and a peak value of 1.76 MW/m^2 at the reactor midplane. The peak value is 60% higher than the average reactor value.

Table 7. Nuclear Heat Loads (kW) in One Quarter of the Element Module for 1 MW/m^2

Component	Neutron Heating	Gamma Heating	Total
Radome	3.962	1.358	5.320
Faraday Shield	2.314	0.995	3.309
Loop	0.433	4.548	4.981
Ground Plane	0.546	7.215	7.761
Loop and Ground Plane Coolant Tubes	1.288	0.732	2.020
SF_6 Gas	0.076	0.036	0.112
Coax	0.460	0.715	1.175
Module Frame	8.523	46.517	55.040
Nuclear Shield	6.474	29.799	36.273

The nuclear radiation environment in the different launcher components has been determined. The peak fast neutron (E > 0.1 MeV) fluence in the BeO radome after one year of full operation is 10^{22} n/cm^2 leading to significant microcracking and strength degradation. Neutron activation calculations have been performed to determine the activity level of the SF_6 gas. A total SF_6 activity of 5 x 10^4 Ci in the four launcher modules needs to be handled after shutdown. One day after shutdown this activity level is reduced by a factor of four. Nuclear heating in SF_6 results in a breakdown rate of 5.9 x 10^{15} molecules/cm^3•s. This extremely high breakdown product production rate requires continuous recirculation through purification systems to remove these corrosive products.

The total nuclear heat load in the four launcher modules amounts to 45 MW. The nuclear heat load to be handled by the loop coolant in one element module is 102 kW. We estimated that a total nuclear shield thickness of 1.6 m is required to allow for hands-on maintenance behind the module one day after shutdown.

Acknowledgments

The SF_6 activation was calculated by A. White. L. Wittenberg provided the information about SF_6 breakdown.

References

1. USA Contribution to the INTOR Phase-Two - A Workshop, Report FED-INTOR/82-1, Georgia Institute of Technology, Atlanta (1982).

2. "MCNP - A General Monte Carlo Code for Neutron and Photon Transport," LA-7396-M, Los Alamos National Laboratory (1981).

3. H. Attaya and M. Sawan, "Neutron Wall Loading Distribution in Toroidal Reactors with General Plasma and First Wall Shapes," to be published as a UWFDM report, University of Wisconsin (1984).

4. R. Wilkes, "Neutron-Induced Damage in BeO, Al_2O_3 and MgO - A Review," J. Nucl. Mat. 26, 137 (1968).

5. T. Sung and W. Vogelsang, "DKR: A Radioactivity Calculation Code for Fusion Reactors," University of Wisconsin Fusion Engineering Program Report UWFDM-170 (1976).

6. T. Ophel et al., "Aspects of Breakdown Product Contamination of Sulphur Hexafluoride in Electrostatic Accelerators," Nuclear Instruments and Methods 217, 383 (1983).

7. J. Spinks and R. Woods, An Introduction to Radiation Chemistry, Wiley, New York, 1976, pp. 232-234.